RESEARCH PAPER

SPATIOTEMPORAL VARIABILITY OF PALMER DROUGHT SEVERITY INDEX INFERRED FROM LONG TREE-RING CHRONOLOGIES IN THE RUSSIAN AND MONGOLIAN PARTS OF THE LAKE BAIKAL BASIN

Saygaa A. Sat*, Alexander A. Ayurzhanaev, Sergey G. Andreev, Bator V. Sodnomov
Baikal Institute of Nature Management of the Siberian Branch of RAS, 6 Sakhyanovoi St., Ulan-Ude, 670047, Russia
***Corresponding author:** saygaa@mail.ru
Received: November 14th 2025 / Accepted: March 31st 2026 / Published: June 30th 2026
https://doi.org/10.24057/2071-9388-2026-4381

ABSTRACT. The spatiotemporal variability of moisture conditions in the Lake Baikal basin, a key region of Inner Asia, remains insufficiently understood due to the short duration of instrumental observations and the complex interplay of climatic factors. In this study, we reconstructed the self-calibrating Palmer Drought Severity Index (PDSI) for May–July using four long tree-ring chronologies from the Russian and Mongolian parts of the Baikal basin. Linear models explain 34–57% of the interannual variance in the instrumental PDSI. The 11-year smoothed mean PDSI values reveal alternating periods of in-phase and out-of-phase moisture variability between the two parts of the basin over the past ~250 years, while long-term (30-year) series show divergent trends: increasing moisture availability in the northern (BRG) and southwestern (HEC) parts of the basin and intensifying aridization in the central-southern part (KST, KRN). Several extreme drought (1863, 1923, and 2003) and wet (1938) years with broad spatial extent were identified. Spectral analysis of the reconstructed series revealed significant cycles of approximately 2–5 years and 14–56 years. The results of this study demonstrate substantial spatial heterogeneity in drought dynamics and highlight the influence of both local and large-scale climatic factors on moisture regimes in Baikal Asia.

KEYWORDS: PDSI reconstruction, dendroclimatology, drought, floods, Baikal Asia

CITATION: Sat S. A., Ayurzhanaev A. A., Andreev S. G., Sodnomov B. V. (2026). Spatiotemporal Variability Of Palmer Drought Severity Index Inferred From Long Tree-Ring Chronologies In The Russian And Mongolian Parts Of The Lake Baikal Basin. Geography, Environment, Sustainability, 2 (19), 96-106
https://doi.org/10.24057/2071-9388-2026-4381

ACKNOWLEDGEMENTS: The work was carried out within the framework of the state task of the Baikal Institute of Nature Management SB RAS FWSU-2026-0009

Conflict of interests: The authors reported no potential conflict of interests.

INTRODUCTION

Climate change in Russia is evidenced by a rate of warming more than twice the global average, a trend expected to continue in the 21st century (Roshydromet 2014; Edelgeriev et al. 2021). Anthropogenic influences are expanding arid zones and intensifying extreme heat and precipitation events. Extreme climatic phenomena – heat waves, droughts, floods, wildfires, etc. – significantly impact ecosystems; in Asia, these effects are especially acute due to high drought vulnerability[1]. However, confidence in drought trend assessments remains low because of limited long-term observations, inconsistent definitions, and spatial heterogeneity. Drought, as a natural phenomenon, lacks clear temporal and spatial boundaries, since its intensity is hard to define and measure (Wilhite and Glantz 1985).

Drought impacts are particularly critical in arid and semi-arid regions. The Lake Baikal basin, spanning parts of Russia and Mongolia, also experiences droughts. A hydrological drought since 1995 has reduced the annual flow of the Selenga River, the main tributary of Lake Baikal. Consequently, suspended sediment transport changed (Chalov et al. 2015; Kasimov et al. 2020), the unique Selenga River delta's barrier functions deteriorated (Chalov et al. 2016; Frolova et al. 2017b), and Lake Baikal's water level regime was disrupted (Alymbaeva et al. 2024).

Regular weather observations in the Russian Baikal basin began in the late 19th century and expanded in the 1930s–1950s. Mongolia's hydrometeorological service started in the mid-20th century. Thus, instrumental data alone cannot fully capture the duration and intensity of historical droughts. Trees with distinct annual rings in harsh climates act as natural "meteorological stations": in arid environments, ring widths closely reflect site moisture and are widely used to reconstruct droughts centuries into the past (Tabakova et al. 2020). For the quantitative assessment of moisture conditions, one of the key indicators is the

[1]IPCC, 2021: Summary for Policymakers. In: Climate Change 2021: The Physical Science Basis. Contribution of Working Group I to the Sixth Assessment Report of the Intergovernmental Panel on Climate Change [Masson-Delmotte, V., P. Zhai, A. Pirani (eds.)]. In Press.

Palmer Drought Severity Index (PDSI), which is widely applied in dendroclimatic reconstructions and reflects a close relationship with tree-ring width in the arid territories of Russia (Kuznetsova and Pozhidaeva 2017; Shigimaga et al. 2024) and Asia (Cook et al. 2010).

Over the past decades, numerous studies have been conducted in the Mongolian part of the Lake Baikal basin to reconstruct moisture variability, river runoff (Davi et al. 2006; Pederson et al. 2001; Leland et al. 2013; Davi et al. 2013), and the PDSI (Davi et al. 2010; Pederson et al. 2014; Haraguchi et al. 2022). In contrast, substantially fewer such studies have been carried out in the Russian part of the basin (Andreev et al. 1999; 2001; Demina et al. 2017; Belokopytova et al. 2018), and studies specifically devoted to PDSI reconstruction based on long chronologies are lacking. At the same time, no previous comparative analysis of the variability of this index across different parts of the Lake Baikal basin has been conducted.

The present study provides the first spatiotemporal reconstruction of the PDSI encompassing the entire Baikal basin. The research objectives are as follows: 1) to reconstruct and compare the history of droughts in the Russian and Mongolian parts; 2) to identify long-term trends and extreme events; 3) to assess the spatial heterogeneity of the moisture regime in different parts of the basin.

MATERIAL AND METHODS

Study Area and Climate

The Lake Baikal basin lies in Inner Asia and covers 545,000 km^2 (excluding the lake area). About 45% of the basin's area is in Russia and 55% in Mongolia. The basin extends over 1300 km from south to north and up to 800 km from west to east at its widest point, in the Mongolian part. The climate of Baikal Asia is sharply continental, with large annual and diurnal temperature ranges and uneven seasonal precipitation. Mean annual air temperatures range from –0.1 °C in the south to –6.7 °C in the north; January is the coldest month, July – the warmest. The mountainous terrain causes complex precipitation patterns: the lowest annual totals (250–400 mm) fall in the steppes and valleys, while the highest totals (>1000 mm) occur in the mountains (e.g., Khamar-Daban Range). Up to 90% of precipitation occurs in summer and autumn as rain, except in the northern basin, where 30–50% is snow (Garmaev 2010).

Vegetation comprises three main types: alpine, boreal (taiga), and steppe. Boreal forests extend far south along ranges, while steppes spread northward through intermontane basins. Forests cover much of the region (mean forest cover ~62.5% in the Russian part vs ~11.5% in the Mongolian part). Coniferous species (pine, larch) dominate, with some birch and aspen (Ecological Atlas… 2015).

Tree-Ring Chronologies

This study uses chronologies from the Barguzin, Uda, and Chikoy river valleys (Russian part) and the Ider Valley (northwestern Mongolia), covering diverse climatic zones of the Baikal basin. We selected the longest available chronologies from forest-steppe sites to maximize drought history coverage (Fig. 1). Sampling and core analysis followed standard dendrochronological methods (Vaganov et al. 1996). We extracted cores from living trees using an increment borer, targeting dominant species in the study area: Scots pine (*Pinus sylvestris L.*) and Siberian larch (*Larix sibirica Ledeb.*). All chronologies were built from cores of living trees collected in 2016–2019 field campaigns, about one-third of which were old-growth individuals.

The KST chronology was extended back to 1498 CE using historical wood from an ethnographic museum building (Andreev et al. 2022). The KRN chronology was extended to 1608 CE using wood from an old house (19th-century heritage site) in the city of Kyakhta.

Ring widths were measured using a LINTAB 5 system with a precision of 0.01 mm. Crossdating and identification of false/missing rings were performed in TSAP-Win; dating quality and statistics were checked with COFECHA software. Series with low coherence were removed based on interseries correlation (Rbar) criteria. All chronologies (including those extended with historical wood) were standardized uniformly: age trends were removed with negative exponential or cubic spline fits (ARSTAN software). We then derived the Tree-Ring Index (TRI) from these standardized series. Residual chronologies (with autocorrelation removed) were used for climate reconstruction, as they preserve high-frequency variations and showed the highest predictive skill in split-period validation.

Chronology quality was evaluated using mean interseries correlation (Rbar), mean sensitivity (MS), standard deviation (SD), and expressed population signal (EPS). EPS was calculated for 51-year windows with 25-year overlap. It indicates periods when sample depth is sufficient for high-accuracy climate reconstruction (common signal exceeds noise), usually requiring EPS > 0.85.

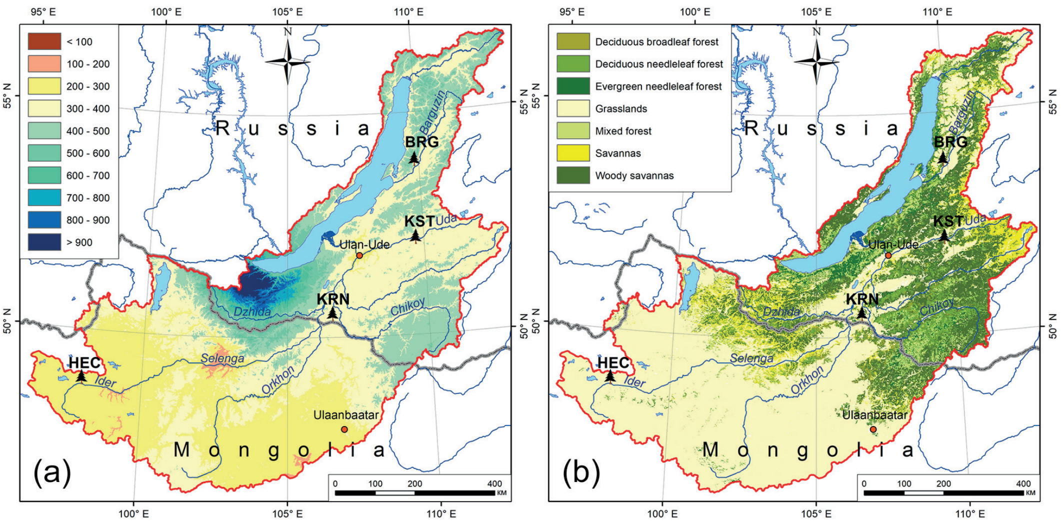

Fig. 1. Study area: (a) mean annual precipitation (mm); (b) landscape types (forest, forest-steppe, steppe, etc.) in the Baikal basin, along with locations of the tree-ring chronologies

Climate Data

We used climatic data from CRU TS 4.06 (0.5° grid, period 1931–2016), obtained via the KNMI Climate Explorer[2]. For each site, mean monthly temperature, precipitation, and the self-calibrating PDSI (scPDSI) were extracted from the grid cells closest to the tree-ring chronologies exhibiting the highest correlations. The PDSI is based on a monthly climatic water balance model, determined by precipitation, temperature, and local soil water-holding capacity (Palmer 1965). The PDSI, derived from CRU TS data, is widely used as a gridded target variable in drought studies (van der Schrier et al. 2013). However, the accuracy of CRU TS depends on the density of the meteorological network; a sparse network can smooth out extremes, reduce variance, and distort trends (Harris et al. 2020). Therefore, the calibration of tree-ring chronologies with PDSI should be interpreted as a response to the grid-cell-averaged moisture signal, rather than as a point-by-point comparison with a specific station. Nevertheless, most of the tree-ring chronology sites are located near meteorological stations, which supports the reliability of the gridded data in representing instrumental records for the region. The analysis was restricted to the post-1931 period to ensure more reliable meteorological data coverage.

Analysis and Reconstruction Methods

Tree-ring width and climate relationships were analyzed with DendroClim 2002 software, using bootstrap confidence intervals for correlation significance. Correlations were computed for the period June of the previous year to August of the current year (accounting for cambial growth timing and prior-year effects).

Climate reconstruction methods follow standard dendrochronological procedures (Fritts 1976; Cook and Kairiukstis 1990). The reconstruction model – a transfer function – is typically a linear regression relating climate parameters to tree-ring indices. The procedure includes model calibration (using observed data), verification, and then actual reconstruction. Model reliability was assessed via split-sample tests, computing statistics: coefficient of determination (adjusted R^2), sign test (ST), reduction of error (RE), and coefficient of efficiency (CE) (Fritts 1976).

Regional representativeness was evaluated by correlating each reconstruction with the gridded PDSI field over 1931–2016. The correlation maps indicate where each series reflects actual PDSI variability. Spectral analysis was conducted with the Multi-Taper Method (MTM), which effectively separates signal from noise in climate time series. We used 5 tapers (3π) and tested against a red-noise background at $p < 0.05$. Morlet wavelet transforms were applied to assess temporal changes in periodicities and phase relationships. Analyses were performed in R Studio and STATISTICA 12.

RESULTS

Tree-ring chronologies and Climate Response

Statistical characteristics of the indexed chronologies are shown in Table 1. All chronologies are suitable for dendroclimatic analysis: Rbar ranges from 0.45 to 0.74, and MS from 0.24 to 0.48, with the highest sensitivity at HEC (driest site) and lowest at BRG (wettest site; see Fig. 1).

The results of the correlation analysis show that precipitation plays an important role in controlling tree-ring width, particularly moisture accumulated in the soil during the second half of the previous growing season (Fig. 2). Precipitation in the current year was also significant for all chronologies during specific summer months. For BRG, located near the shore of Lake Baikal, significant relationships were found with January precipitation (snow) and warm conditions in October of the previous year. This likely reflects the influence of the lake-modified microclimate of Baikal (Mizandrontseva 1985).

Air temperature at the southernmost site (HEC, northwestern Mongolia) showed predominantly negative relationships with radial growth, which likely reflects an indirect moisture-mediated effect: under semiarid conditions, higher temperatures enhance evapotranspiration and intensify soil moisture deficit, thereby constraining tree growth (Liu et al. 2019). All chronologies showed significant positive correlations with PDSI, with the highest coefficients observed for BRG. Overall, the strongest correlations for all chronologies were observed in May–June.

PDSI Reconstruction and Validation

Based on the TRI – climate relationships, we selected the current-year mean May–July PDSI for reconstruction.

Table 1. Statistical characteristics of chronologies

Parameter	BRG	KST	KRN	HEC
Tree samples	33	74	118	20
Tree species	PISY, LASI	PISY	PISY	LASI
Period, year	1541–2019	1498–2016 (1699–1998*)	1608–2017 (1797–2017)*	1574–2018
Duration	479	519	410	445
Rbar	0.45	0.74	0.64	0.70
MS	0.24	0.35	0.34	0.48
SD	0.31	0.61	0.41	0.51
EPS > 0.85	1688–2019	1530-2016	1631–2017	1763–2018

*The range of the initial chronology of KST and KRN.

[2]https://climexp.knmi.nl/

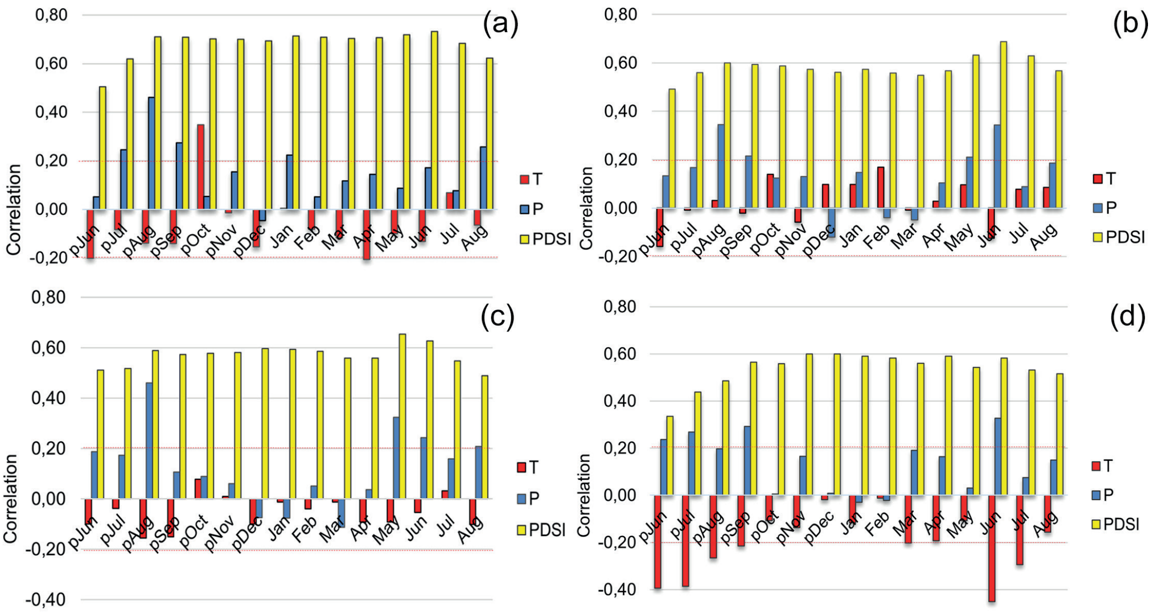

Fig. 2. Correlation of tree-ring chronologies: (a) BRG, (b) KST, (c) KRN, and (d) HEC with average monthly air temperature (T), precipitation amount (P) and PDSI for the period 1931–2016. Dotted red lines indicate the level of statistical significance ($p < 0.05$)

Model performance was evaluated by comparing observed and modeled PDSI using adjusted R^2 (Table 2). To assess predictive skill, the instrumental period was divided into two equal sub-periods for calibration and verification. Sub-period cross-validation demonstrated the stability of the regression models. The Sign Test (ST) indicated a significant excess of agreements, confirming that tree-ring variability captured PDSI variability. The positive values of the RE and CE statistics for all verification periods indicate that the reconstructions exhibit significant predictive skill. Overall, the models performed well: BRG explains 57% of the variance in PDSI, KST 46%, KRN 37%, and HEC 34% for 1931–2016. The linear regression equations relating TRI to instrumental PDSI over the full instrumental period are as follows (Eqs. 1–4):

$$PDSI_{BRG} = 12.51 \times TRI - 11.81 \quad (1)$$

$$PDSI_{KST} = 5.33 \times TRI - 4.51 \quad (2)$$

$$PDSI_{KRN} = 4.95 \times TRI - 4.44 \quad (3)$$

$$PDSI_{HEC} = 3.22 \times TRI - 3.85 \quad (4)$$

Table 2. Statistics of split calibration and verification models for reconstructing the average PDSI value from May to July according to tree-ring chronologies

Calibration		Verification			
Period	R^2adj	Period	ST	RE	CE
BRG					
1931–1973	0.49	1974–2016	32+/11	0.70	0.49
1974–2016	0.49	1931–1973	36+/7-	0.75	0.48
1931–2016	0.57	1931–2016	67+/19-		
KST					
1931–1973	0.58	1974–2016	32+/11-	0.56	0.36
1974–2016	0.44	1931–1973	31+/12-	0.67	0.44
1931–2016	0.46	1931–2016	64+/22-		
KRN					
1931–1973	0.44	1974–2016	27+/16-	0.54	0.23
1974–2016	0.34	1931–1973	36+/7-	0.60	0.33
1931–2016	0.37	1931–2016	59+/27-		
HEC					
1931–1973	0.26	1974–2016	33+/10-	0.47	0.35
1974–2016	0.37	1931–1973	29+/14-	0.49	0.09
1931–2016	0.34	1931–2016	67+/19-		

Fig. 3a shows the reconstructed May–July PDSI series for all four sites. The series clearly reflect local moisture regime differences. In the northern region (BRG, KST), wetter phases dominate: mean PDSI values for the full reconstruction are 0.74 (BRG) and 0.82 (KST). In the central and southern basin (KRN, HEC), mean values are 0.53 and –0.66, indicating pronounced aridity, especially at HEC (NW Mongolia).

To examine long-term fluctuations, smoothed series were computed using 11- and 30-year moving averages (Figs. 3b, c). The 11-year smoothed series indicate shifts in synchrony: prior to the 1870s, moisture variations in the Russian and Mongolian sectors were mostly asynchronous; during ~1870–1980 in-phase and lagged phases alternated; after the 1980s, an asynchronous regime resumed (Fig. 3b). Notably, PDSI values converged in the late 20th century. The 30-year smoothed series (253 years long, EPS > 0.85 since 1763) show divergent trends: Uda and Chikoy basins (KST, KRN) show a drying trend (decreasing PDSI), while Barguzin and Ider (BRG, HEC) show a wetting trend (increasing PDSI). HEC, however, remains below zero (never surpassing its long-term mean) (Fig. 3c).

Spatial correlation patterns

Fig. 4 shows maps of correlations between each reconstruction and observed PDSI (CRU TS) for 1931–2016. All reconstructions exhibit significant positive correlations over broad areas, indicating good representativeness. BRG has the largest area of correlation: high coefficients ($r \approx 0.3–0.7$, $p < 0.05$) cover coastal Baikal, western Transbaikalia, and part of the Eastern Sayan. KST shows a strong correlation over Western Transbaikalia and parts of Eastern Transbaikalia. HEC correlates highly with grid cells across the Mongolian part of the Lake Baikal basin. The highest correlation for KRN is observed in the border areas of Russia and Mongolia. These results confirm that the reconstructions reliably capture spatial climate variability.

Extreme Dry and Wet Periods

The long reconstructions (EPS > 0.85; 250–480 years) enable identification of the most prolonged drought and pluvial periods in each part of the basin (Fig. 3a). Drought periods are sequences of years with negative PDSI, and wet periods are those with positive PDSI. In the Barguzin Valley (BRG), droughts were observed in 1797–1809 and 1977–1984 and a wet period in 1925–1942. In the Uda Basin (KST), two 8-year droughts occurred: 1730–1737 and 1838–1845 (the latter more severe, including the driest year, 1838); wet periods were 1740–1760, 1926–1943, 1983–2002. In the border part (KRN), a drought occurred in 1648–1655 (including extreme 1650), followed by droughts in 1728–1738, 1954–1961, 1977–1984, and a wet period in 1865–1887. In NW Mongolia (Ider Valley, HEC), a drought occurred in 1769–1792. The 19th century featured the longest droughts: 1808–1843 and 1847–1869, with the peak wet interval of the entire record occurring between these mega-droughts (1793–1807).

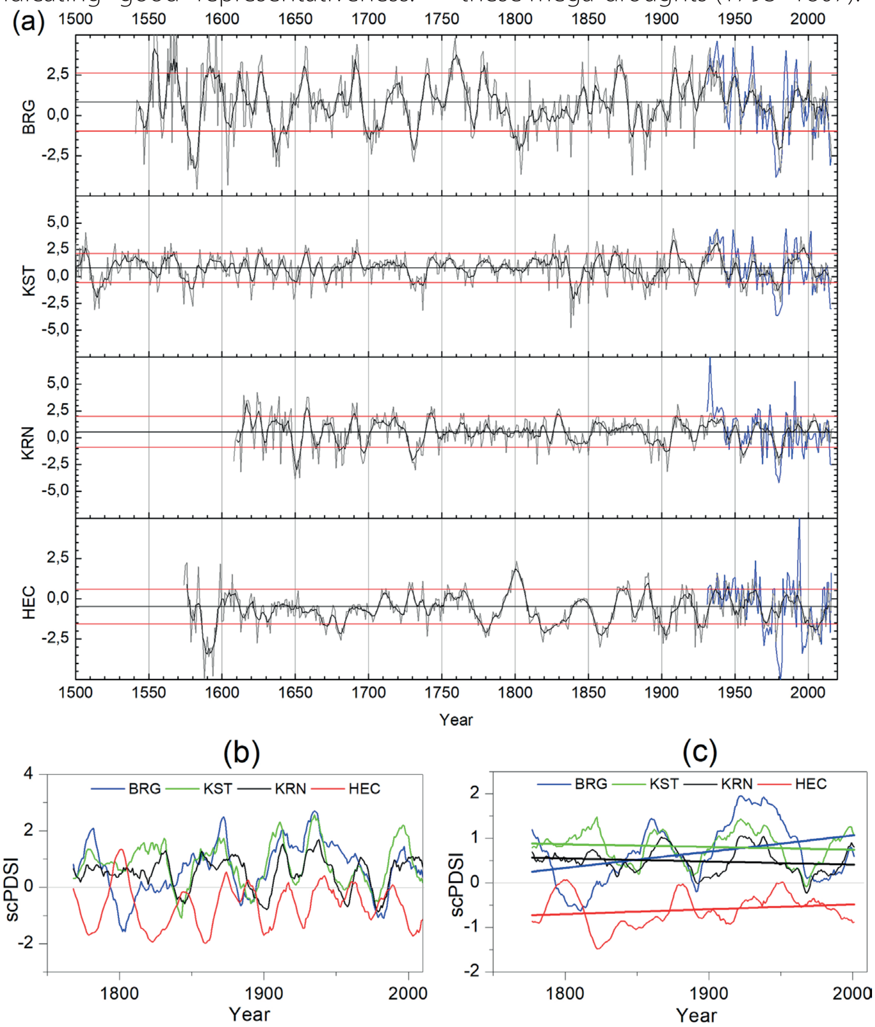

Fig. 3. Reconstruction of the average PDSI for May–July: (a) complete reconstruction for the four study sites (gray – reconstructed series; blue – instrumental data; black – 5-year moving average; red – ±1 SD); (b) 11-year moving average; (c) 30-year moving average. Moving averages are shown for the common interval beginning in 1763, when EPS exceeded 0.85 for all chronologies

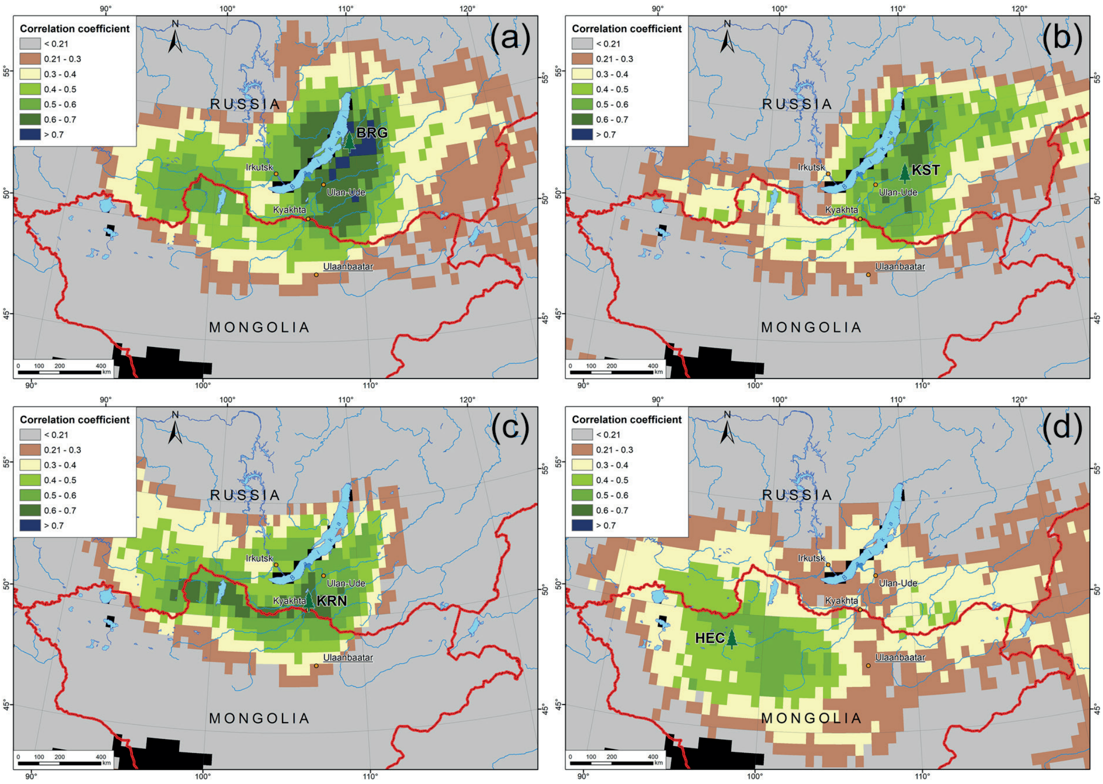

Fig. 4. Maps of spatial correlation between reconstructed and actual PDSI (1931–2016): (a) BRG, (b) KST, (c) KRN, and (d) HEC. The correlations are statistically significant at r > 0.21 (p < 0.05)

Extreme hydroclimatic events cause significant damage to ecosystems, agriculture, and economies, making their frequency important to understand. Extremely dry and wet years (below the 5th and above the 95th percentiles of PDSI) are listed in Table 3 for periods with EPS > 0.85. Some extremely dry and wet years affected broad areas across Baikal Asia – from the northern to the southern parts, as reflected in synchronous dry years (1863, 1923, 2003) and a synchronous wet year (1938).Our reconstructions and extremes align with previous studies. The negative extremes 1801, 1838, 1840 and the positive 1827–1830 coincide with Selenga River flow reconstructions (Andreev et al. 2001; Belokopytova et al. 2018; Demina et al. 2022). The HEC series (NW Mongolia) also matches prolonged drought and wet periods in west-central Mongolia (Davi et al. 2006) and certain common phases spanning central and eastern Mongolia (Pederson 2001; 2014; Davi et al. 2010; 2013). The late 18th–early 19th centuries exhibit spatial asynchrony: the central-western basin was wetter compared to the eastern basin (Davi et al. 2006). Our data confirm such out-of-phase regimes: during this period, the Mongolian part was anomalously wet, whereas the northern part of the basin experienced extreme droughts (1800–1805 period ranks among the driest years). In the modern era, a similar asynchrony is seen in the events of 1984, 2014 and 2016–2017 (based on the 10th and 90th percentile thresholds).

The reconstructed extreme years were compared with natural chronicles from Transbaikalia and Mongolia (Zadonina and Levi 2008) to validate the results for the pre-instrumental period, including asynchronous phases. The chronicles confirm, for example, the forest fires in the Barguzin Valley in 1804, and in the asynchronous year 1889 a severe drought occurred in Barguzin, while Cisbaikalia and eastern Transbaikalia simultaneously experienced flooding. Some events did not coincide, as chronicles more often describe regional-scale catastrophes rather than local ones.

During the recent asynchronous period of 2016–2017, the northern part experienced the largest forest-cover losses in 20 years due to wildfires, which were preceded by spring-summer droughts (Tsydypov et al. 2022). In the same years, catastrophic floods caused by heavy rains were recorded in the northwestern and western aimags of Mongolia (Serdyanjiv et al. 2024). In Khovd, total annual and summer precipitation has decreased by ~20% over the past 40 years, yet extreme downpours have become more frequent. Among such anomalously wet years, the asynchronous year 1984 stands out, when up to 85% of the annual precipitation norm fell within a single season in some locations (Narangerel et al. 2025).

Spectral and Wavelet Characteristics

Fig. 5 shows power spectra and Morlet wavelet spectra for all four PDSI series (p < 0.05). High-frequency peaks appear in all series: BRG ~2.2–2.3 years; KST ~2–5 years; KRN ~2.2–2.6 years; HEC ~2.4–3.6 years. Low-frequency oscillations (multi-decadal) are most pronounced in KST and HEC. KST has persistent cycles of ~26–36, ~46.5, ~48.7 years; HEC has ~26.9–36.6, ~39.4, ~42.7, ~46.5, ~51.2, ~56.8 years. KRN shows significant power at ~14–17, ~23–27, ~33 years. These periods match the Pacific Decadal Oscillation (PDO) timescales (~20–30, 50–70 years). The ~14–17 year cycle in KRN is consistent with the ~18–year lunar nodal cycle.

Wavelet analysis confirmed the main intra-centennial periodicities identified by the MTM method. In addition to high-frequency oscillations, the BRG chronology exhibited a pronounced low-frequency cycle with a period of ~16–22 years. This periodicity is consistent with the Hale solar cycle and was particularly evident from the 1720s to the 1770s. A common ~26–48-year cycle was simultaneously observed in KST and HEC throughout approximately the 1800s–1950s. Of note, the power of the 50–60-year periodicities in KST is weakly expressed. In KRN, ~14–17-year cycles were recorded around 1650–1720, followed by dominant ~23–33-year oscillations in 1720–1750. An approximately 32-year common cycle was identified in both KST and HEC during 1920–1970.

Table 3. Extremely dry and wet years in the reconstructed PDSI

BRG		KST		KRN		HEC	
5P	95P	5P	95P	5P	95P	5P	95P
		1556, 1574, 1579–1580	1561, 1565				
	1689, 1692–1693	1620, **1649–1650**, 1661, 1671	1617, 1627, **1657, 1689, 1692**	1640, **1649–1651**, 1653, 1666 1678, 1682–1683, 1696–1697	1634, 1638–1639, 1643, 1647, **1657**–1659, **1689**–1690, **1692**		
1702, **1730–1731**	1740, 1758–1760, 1762, 1777–1778	1737	–	**1730–1732**	1711, 1717, 1719, 1743, 1745	1780	1798–1799
1801, 1804–1805, 1809, 1829, 1838, 1880, 1889	1871	**1838**, 1840, 1843–1844, 1850, **1863**, 1888–1889, 1892	1826–1827, 1836, 1856, 1860, 1867, 1870	1815, 1893, 1898	1829–1830	1819, 1858–1859, **1863**	1800–1805, 1889–1891
1980–1982	**1908–1909**, 1921, 1932–1933	**1923**, 1954–1955, 1958, 1969, **1981**	**1907–1910**, 1932–**1933**, 1937–**1938**, 1995, 1997	1904, **1954**, **1980**	1911–1912	1901, 1903, **1923**, 1927, 1978	**1938**–1939, 1944, 1962
2003, 2016, 2019	–	2006	–	–	–	**2003**, 2008	–

Note: Synchronous dry or wet years are highlighted in bold; asynchronous years are marked with a dash.

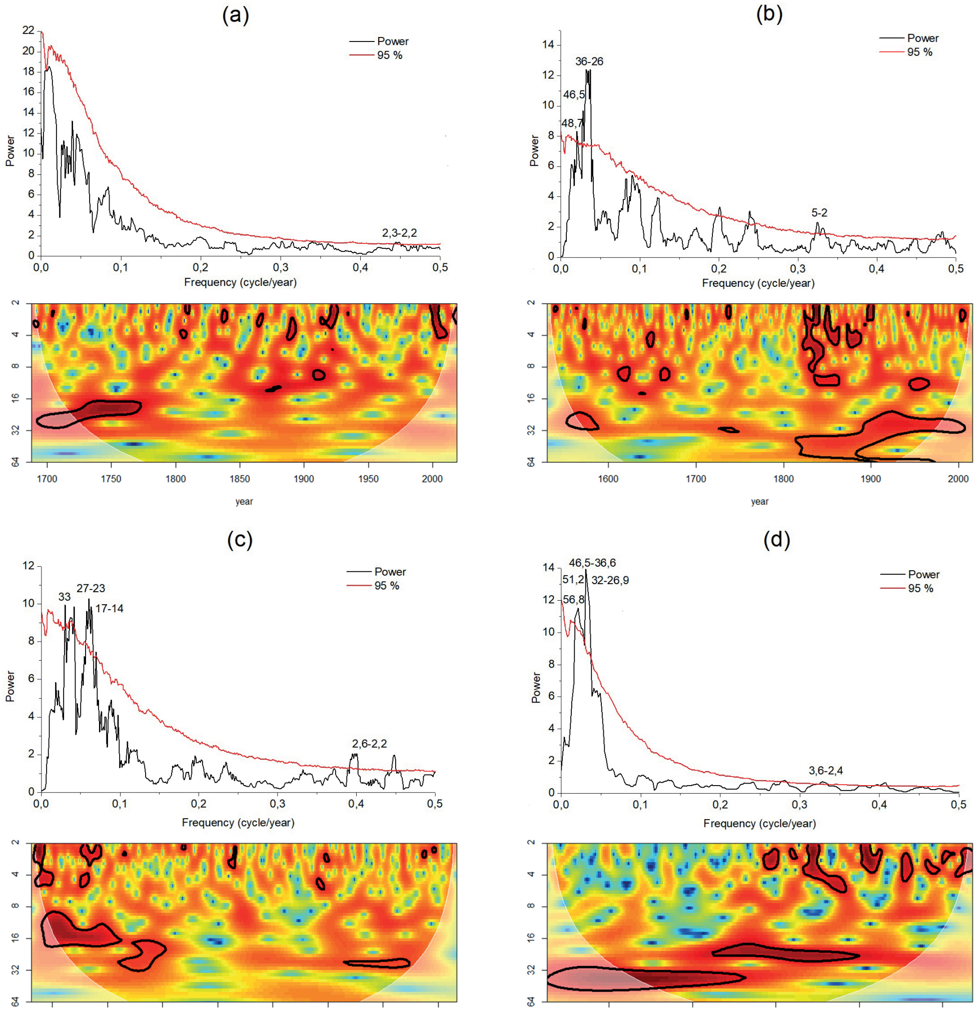

Fig. 5. Spectral power of the series: (a) BRG, (b) KST, (c) KRN, (d) HEC ($p < 0.05$) obtained by the multitaper method and their Morlet wavelets

Synchrony and Asynchrony Between Regions

Because the fluctuations can be both synchronous and asynchronous, we calculated running correlations for each pair of reconstructed PDSI series for 1763–2016 (EPS > 0.85 for the common interval), using 11- and 30-year windows with a 1-year step. Correlation values range from negative values (indicating antiphase) to positive values (indicating in-phase behavior). The results (Fig. 6) clearly illustrate the sequence of synchronous and asynchronous intervals over the past 253 years.

The 11-year running correlations (Fig. 6a) show that among the chronologies BRG, KST, and KRN (Russian part of the basin), positive relationships dominate, with only occasional negative episodes. Between the Russian and the Mongolian PDSI series, phases of synchrony and antiphase regularly alternate; correlation coefficients vary approximately from –0.8 to 0.8 (Fig. 6b).

In the 30-year window, the synchrony among the Russian PDSI series strengthens during the 20th century, especially between BRG and KRN (Fig. 6a). Correlations between the Russian and the Mongolian series, which were predominantly negative until the late 19th century, shift toward positive values by the mid-20th century: in the second half of the 20th century, all chronologies demonstrate persistent in-phase behavior (Fig. 6b).

Cross-wavelet analysis of the series (Fig. 7) reveals coherent variations across multiple temporal scales. For pairs of Russian part chronologies, the phases of oscillations within the significant regions of the spectrum predominantly coincide (arrows →), or one series slightly leads the other by π/2 (↗/↘) (Fig. 7a). It was found that in the KST, KRN, and HEC PDSI reconstruction series, persistent low-frequency (multidecadal) oscillations are present throughout the entire interval, with phase arrows transitioning from antiphase through intermediate phase shifts to in-phase behavior and then back to antiphase (with some episodes falling outside the cone of influence). High-frequency (interannual) coherence between the Russian and Mongolian series appears only from the late 19th century onward (Fig. 7b).

Between the BRG and HEC series, in-phase oscillations are detected only during ~1860–1880 (with a ~22-year cycle); in subsequent years, low-frequency coherence is absent. The presence of a common ~32-year cycle allows it to be linked to the Pacific Decadal Oscillation previously documented for the Russian (Demina et al. 2017) and Mongolian (Davi et al. 2010) sub-basins. The absence of pronounced low-frequency variations in the Barguzin chronology is likely explained by the orographic isolation of Lake Baikal, which is shielded from the west and east by mountain ranges that block the intrusion of near-surface Pacific and Atlantic air masses (Mizandrontseva 1985).

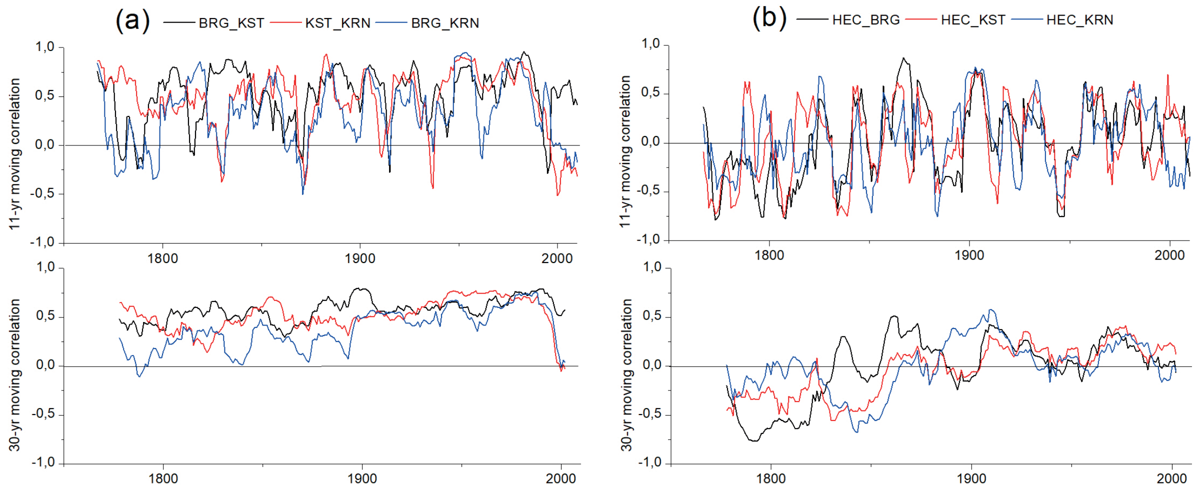

Fig. 6. Running correlations between reconstructed PDSI series calculated using 11- and 30-year moving windows: (a) among the Russian series; (b) between the Mongolian and Russian series

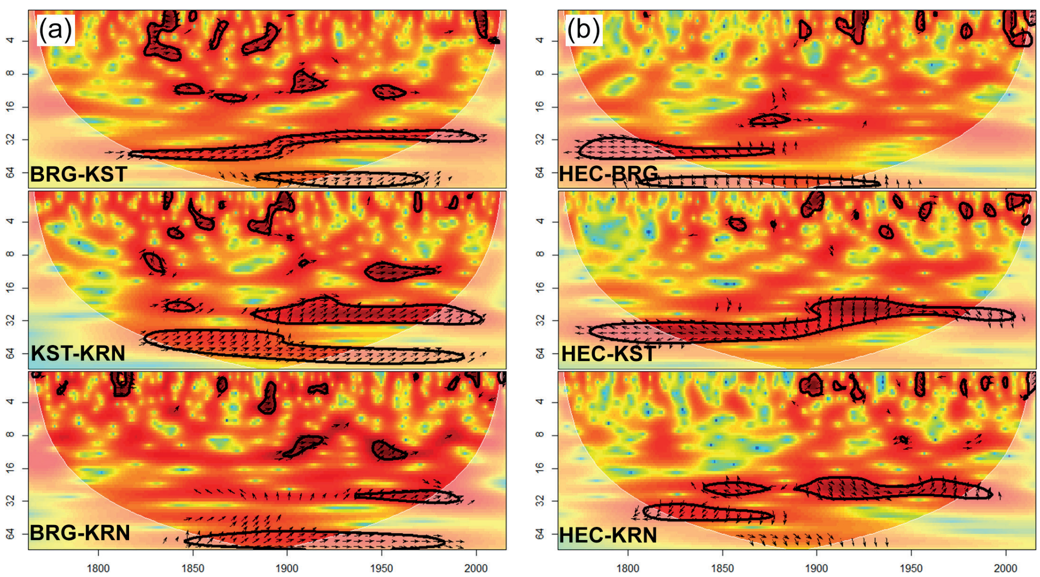

Fig. 7. Cross-wavelet of reconstructed PDSI series for the period 1763–2016, arrows (→ in phase, ← – out of phase, ↗/↘ – advance/delay), the white line indicates the cone of influence: (a) between the PDSI series of the Russian part of the basin, and (b) between the PDSI series of the Mongolian part of the basin and the Russian part

DISCUSSION

The results show that the chronologies from the Russian territory are periodically synchronous and asynchronous with those from northwestern Mongolia, reflecting the influence of both local orographic factors and large-scale atmospheric processes of southern Siberia (Voropay and Ryazanova 2023). Local blocking anticyclones over eastern Siberia and the Mongolian Plateau play a significant role in shaping the precipitation regime (Antokhina et al. 2019; 2023).

Mean values of the reconstructed PDSI demonstrate a climatic gradient from the humid north to the semi-arid south. The 11-year smoothed PDSI values indicate similar climatic conditions during the second half of the 20th century in the valleys of the Uda, Chikoy, and Ider rivers. Long-term 30-year trends (1763–2016) show decreasing moisture availability (increasing aridity) in the Uda and Chikoy valleys and increasing moisture availability in the Barguzin and Ider basins. These findings are consistent with reconstructions of multidecadal streamflow variability of the lower Selenga (Andreev et al. 2001; Belokopytova et al. 2018) and its upper reaches (Davi et al. 2006). Recent hydrological studies from the Selenga basin also indicate spatially heterogeneous runoff changes under recent warming (Frolova et al. 2017). Notably, modern droughts in Mongolia, although extreme, are not unprecedented within the multi-millennial context of climate reconstructions for Central Asia (Hessl et al. 2018).

These regional trends align with global aridification dynamics. According to Sardans et al. (2024), between 1960 and 2023 approximately 28% of global land areas became drier, while ~20.5% became wetter. In the study by Gelfan et al. (2021), for the period 1976–2016 compared with 1950–1975, the streamflow regime of rivers flowing into Baikal changed: discharge increased in the northern tributaries of the lake (from the Turka River and northward), as well as in the upper Selenga tributaries (the Selenga and Delgermuren rivers), whereas discharge decreased in the lower tributaries (Uda, Chikoy, Khilok rivers). Our reconstructions are broadly consistent with these patterns.

The observed strengthening of synchrony among the Baikal basin tree-ring series is consistent with the global trend of increasing tree-growth synchrony, attributed to the intensification of shared climatic influences (Shestakova et al. 2016; Wang et al. 2021; Li et al. 2024). In particular, synchrony tends to increase in regions with pronounced moisture deficit, where drought is the primary limiting factor of growth (Gazol et al. 2020; Tejedor et al. 2020), whereas in the Mediterranean region, severe droughts instead lead to desynchronization of growth (Sangüesa-Barreda et al. 2019). Despite the increase in regional (a) synchrony, substantial spatial heterogeneity persists. This heterogeneity manifests in high-frequency growth fluctuations and is driven by local site conditions and species composition (Shestakova et al. 2019; Dolgova et al. 2019), which may reduce synchrony and modify growth sensitivity (Muffler et al. 2020).

A comparison of tree-ring data from adjacent regions of the Pacific coast reveals coherence of climatic fluctuations at multidecadal scales (Fang et al. 2018). Results of spectral and wavelet analyses show common low-frequency (~32-year) PDSI oscillations in the tributary basins of the Selenga River, indicating the influence of Pacific processes even on remote inland territories. The detected 14–17-year cyclicity in the border region of the study area corresponds to ~18-year lunar nodal cycles documented in the Minusinsk Basin and on the Mongolian Plateau (Demina et al. 2022; Davi et al. 2010). Thus, the microclimate of the Baikal basin responds sensitively to both local factors and global atmospheric processes. Tree-ring chronologies confirm their value as indicators of large-scale climatic phenomena.

Modern warming driven by increasing greenhouse gas concentrations, together with variability in Pacific and Atlantic ocean-atmosphere systems, may substantially influence future drought dynamics in Inner Asia (Dai 2021; Davi et al. 2010; Wang et al. 2022).

CONCLUSION

In this paper, we reconstructed multi-century changes of the Palmer Drought Severity Index for the transboundary territory of the Lake Baikal basin, reflecting both local climates and connections to large-scale atmospheric processes. A drought tendency was identified for the central-southern territories (KST, KRN) in the basins of the Uda and Chikoy rivers, whereas the opposite trend, i.e., increasing moisture availability, is observed in the northern part (BRG) and in northwestern Mongolia (HEC), in the basins of the Barguzin and Ider rivers.

Promising avenues for future research include analyzing the spatial synchrony and asynchrony of climatic signals in other parts of the Lake Baikal basin and examining the teleconnection mechanisms driving these differences across multiple temporal scales. This will provide a stronger basis for understanding drought and moisture dynamics in the Lake Baikal basin, which contains the world's largest reservoir of liquid freshwater and is experiencing warming faster than the global average.

REFERENCES

Alymbaeva Zh. B., Andreeva A.M., Ayurzhanaev A.A., Ayusheeva S.N., Bardakhanova T.B., et al. (Eds.) (2024). Impact of the Changing Water Level of Lake Baikal on the Economy and Ecosystems. Novosibirsk: Siberian Branch of the Russian Academy of Sciences, Baikal Institute of Nature Management, SB RAS. ISBN 978-5-6050995-5-0. DOI:10.53954/9785605099550.

Andreev S.G., Vaganov E.A., Naurzbaev M.M., and Tulokhonov A.K. (1999). Registration of long-term variations in atmospheric precipitation, Selenga River runoff, and Lake Baikal level by annual pine tree rings. Doklady Earth Sciences, 368(5), 1008–1011. (Transl. from Doklady RAN, 369(6), 825–828).

Andreev S.G., Vaganov E.A., Naurzbaev M.M., and Tulokhonov A.K. (2001). Radial growth of trees as an indicator of long-term changes in the hydrological regime in the Lake Baikal basin. Geography and Natural Resources, (4), 49–54. (In Russian).

Andreev S.G., Ayurzhanaev A.A., Batotsyrenov E.A., et al. (2022). Dendrochronological study of a 19th-century staging barn (Ethnographic Museum of the Peoples of Transbaikalia, Ulan-Ude). Journal of Siberian Federal University. Biology, 15(2), 279–292. https://doi.org/10.17516/1997-1389-0387 (In Russian).

Antokhina O.Y., Antokhin P.N., Martynova Y.V., and Mordvinov V.I. (2019). The linkage of precipitation in the Selenga River Basin to midsummer atmospheric blocking. Atmosphere, 10(6), 343. https://doi.org/10.3390/atmos10060343

Antokhina O., Antokhin P., Gochakov A., Zbirannik A., and Gazimov T. (2023). Atmospheric circulation patterns associated with extreme precipitation events in Eastern Siberia and Mongolia. Atmosphere, 14(3), 480. https://doi.org/10.3390/atmos14030480

Belokopytova L., Zhirnova D., Kostyakova T., and Babushkina E. (2018). Dynamics of moisture regime and its reconstruction from a tree-ring width chronology of Pinus sylvestris in the downstream Selenga basin, Russia. Journal of Arid Land, 10, 877–891. https://doi.org/10.1007/s40333-018-0025-y

Cook E.R. and Kairiukstis L.A. (1990). Methods of Dendrochronology. Applications in the Environmental Sciences. International Institute for Applied Systems Analysis. Kluwer Academic Publishers, Dordrecht, 394 p. http://dx.doi.org/10.1007/978-94-015-7879-0

Cook E.R., Anchukaitis K.J., Buckley B.M., D'Arrigo R.D., Jacoby G.C., Wright W.E. (2010). Asian monsoon failure and megadrought during the last millennium. Science 328, 486–489. https://doi.org/10.1126/science.1185188

Chalov S.R., Jarsjö J., Kasimov N.S., et al. (2015). Spatio-temporal variation of sediment transport in the Selenga River Basin, Mongolia and Russia. Environmental Earth Sciences, 73, 663–680. https://doi.org/10.1007/s12665-014-3106-z

Chalov S., Thorslund J., Kasimov N.S., et al. (2016). The Selenga River delta: A geochemical barrier protecting Lake Baikal waters. Regional Environmental Change, 17(7), 2039–2053. https://doi.org/10.1007/s10113-016-0996-1

Dai A. (2021). Hydroclimatic trends during 1950–2018 over global land. Climate Dynamics, 56, 4027–4049. https://doi.org/10.1007/s00382-021-05684-1

Davi N.K., Jacoby G.C., Curtis A.E., and Baatarbileg N. (2006). Extension of drought records for Central Asia using tree rings: West-central Mongolia. Journal of Climate, 19(2), 288–299. https://doi.org/10.1175/JCLI3621.1

Davi N.K., Jacoby G.C., Fang K., et al. (2010). Reconstructing drought variability for Mongolia based on a large-scale tree-ring network: 1520–1993. Journal of Geophysical Research: Atmospheres, 115(D22), D22103. https://doi.org/10.1029/2010JD013907

Davi N.K., Pederson N., Leland C., Nachin B., Suran B., and Jacoby G.C. (2013). Is eastern Mongolia drying? A long-term perspective of a multidecadal trend. Water Resources Research, 49(1), 151–158. https://doi.org/10.1029/2012WR011834

Demina A.V., Belokopytova L.V., Andreev S.G., et al. (2017). Radial increment dynamics of Scots pine (Pinus sylvestris L.) as an indicator of hydrothermal regime of the Western Transbaikalia forest steppe. Contemp. Probl. Ecol. 10, 476–487. https://doi.org/10.1134/S1995425517050031

Demina A.V., Belokopytova L.V., Zhirnova D.F., Mehrotra N., Shah S.K., Babushkina E.A. and Vaganov E.A. (2022). Degree of connectivity in reconstructed precipitation dynamics and extremes for semiarid regions across South Siberia. Dendrochronologia, 71, 125903. https://doi.org/10.1016/j.dendro.2021.125903

Dolgova E.A., Solomina O.N., Matskovsky V.V., Dobryansky A.S., Semenyak N.A., and Shpunt S.S. (2019). Spatial variation of pine tree-ring growth in the Solovetsky Islands. Izvestiya RAN. Seriya Geograficheskaya, 2, 41–50. https://doi.org/10.31857/S2587-55662019241-50 (In Russian, with English summary).

Ecological Atlas of Lake Baikal. (2015). Irkutsk: SB RAS Press, 145 p. (In Russian).

Edelgeriev R.S.-Kh., Ivanov A.L., Donnik I.M., et al. (2021). Global climate and the soil cover of Russia: Manifestations of drought, prevention, mitigation, elimination of consequences, and adaptation measures (agriculture and forestry). Moscow: MBA Publishing, 700 pp. (In Russian).

Fang K., Cook E., Guo Z., Chen D., Ou T., and Zhao Y. (2018). Synchronous multi-decadal climate variability of the whole Pacific areas revealed in tree rings since 1567. Environmental Research Letters, 13, 024016. DOI 10.1088/1748-9326/aa9f74

Fritts H.C. (1976). Tree Rings and Climate. London: Academic Press, 567 pp.

Frolova N.L., Belyakova P.A., Grigor'ev V.Y., Sazonov A.A., Zotov L.V., and Jarsjö J. (2017). Many-year variations of river runoff in the Selenga basin. Water Resources, 44, 359–371. https://doi.org/10.1134/S0097807817030101

Frolova N.L., Belyakova P.A., Grigoriev V.Yu., Sazonov A.A., Zotov L.V., and Jarsjö J. (2017b). Runoff fluctuations in the Selenga River Basin. Regional Environmental Change, 17, 1965–1976. https://doi.org/10.1007/s10113-017-1199-0

Garmaev E.Zh. (2010). Drainage of the Rivers of the Lake Baikal. - Ulan-Ude: Buryat State University Publishing Department, 272 p. (In Russian).

Gazol A., Camarero J.J., Sangüesa-Barreda G., Serra-Maluquer X., Sánchez-Salguero R., Coll L., and Casals P. (2020). Tree species are differently impacted by cumulative drought stress and present higher growth synchrony in dry places. Frontiers in Forests and Global Change, 3:573346. doi: 10.3389/ffgc.2020.573346

Gelfan A., Frolova M., Magritsky D., Kireeva M., Grigoriev V., Motovilov Yu., and Gusev E. (2021). Climate change impact on annual and maximum runoff of Russian rivers: diagnosis and projections. Fundamental and Applied Climatology, 7(1), 36–79. (In Russian).

Haraguchi M., Davi N., Rao M. P., Leland C., Watanabe M., and Lall U. (2022). Estimating return intervals for extreme climate conditions related to winter disasters and livestock mortality in Mongolia. Natural Hazards and Earth System Sciences, 22(8), 2751–2770. https://doi.org/10.5194/nhess-22-2751-2022

Harris I., Osborn T.J., Jones P. et al. (2020). Version 4 of the CRU TS monthly high-resolution gridded multivariate climate dataset. Sci Data 7(1), 109. https://doi.org/10.1038/s41597-020-0453-3

Hessl A.E., Anchukaitis K.J., Jelsema C., et al. (2018). Past and future drought in Mongolia. Science Advances, 4(3), e1701832. https://doi.org/10.1126/sciadv.1701832

Kasimov N.S., Shinkareva G., Lychagin M., Chalov S., Pashkina M., Thorslund J., and Jarsjö J. (2020). River water quality of the Selenga–Baikal Basin. Part II—Metal partitioning under different hydroclimatic conditions. Water, 12(9), 2392. https://doi.org/10.3390/w12092392

Kuznetsova V.V., Pozhidaeva D.S. (2017). Possibilities and limitations of reconstruction of river flow and aridity conditions in the Volga region by dendrochronological methods. Fundamental and Applied Climatology, 4, 46-65. DOI: 10.21513/2410-8758-2017-4-46-65 (In Russian).

Leland C., Pederson N., Nachin B., Hessl A., Saladyga T., and Suran B. (2013). A hydroclimatic regionalization of central Mongolia as inferred from tree rings. Dendrochronologia, 31(3), 205–215. https://doi.org/10.1016/j.dendro.2012.11.003

Li W., Jiang Y., Lin Z., Wang J., Zhang Y., and Ma W. (2024). Warming-driven increased synchrony of tree growth across the southernmost part of the Asian boreal forests. Science of the Total Environment, 938, 173389. https://doi.org/10.1016/j.scitotenv.2024.173389

Liu Y., Song H., Lei Y., et al. (2019). The 600-mm precipitation isoline distinguishes tree-ring-width responses to climate in China. National Science Review, 6(2), 359–368. https://doi.org/10.1093/nsr/nwy101

Mizandrontseva K.N. (1985). Climate of Lake Baikal in weather patterns. Novosibirsk: Nauka, 160 pp. (In Russian).

Muffler L., Weigel R., Hacket-Pain A.J., Klisz M., van der Maaten E., Wilmking M., Kreyling J., and van der Maaten-Theunissen M. (2020). Lowest drought sensitivity and decreasing growth synchrony towards the dry distribution margin of European beech. Journal of Biogeography, 47(9), 1910–1921. DOI:10.1111/jbi.13884

Narangerel S., Suzuki Y., Taniguchi K., et al. (2025). Floods and related problems after the 1980s in Khovd, Western Mongolia. Nat. Hazards, 121, 23627–23646. https://doi.org/10.1007/s11069-024-07033-x

Palmer W.C. (1965). Meteorological drought, Res. Pap., 45, U.S. Dept. of Commer. Weather Bur., Washington, D. C.

Pederson N., Jacoby G.C., D'Arrigo R.D., Cook E.R., Buckley B.M., Dugarjav C., and Mijiddorj R. (2001). Hydrometeorological reconstructions for northeastern Mongolia derived from tree rings: AD 1651–1995. Journal of Climate, 14(5), 978-991. https://doi.org/10.1175/1520-0442(2001)014<0872:HRFNMD>2.0.CO;2

Pederson N., Hessl A.E., Baatarbileg N., Anchukaitis K.J., and Di Cosmo, N. (2014). Pluvials, droughts, the Mongol Empire, and modern Mongolia. Proceedings of the National Academy of Sciences of the United States of America, 111(12), 4375-4379. https://doi.org/10.1073/pnas.1318677111

Roshydromet. (2014). Second Roshydromet Assessment Report on Climate Change and Its Consequences for the Russian Federation. Moscow: Roshydromet, 1004 pp. (In Russian).

Sangüesa-Barreda G., Camarero J.J., Sánchez-Salguero R. et al. (2019). Droughts and climate warming desynchronize Black pine growth across the Mediterranean Basin. Science of the Total Environment, 697. 133989. DOI: 10.1016/j.scitotenv.2019.133989

Sardans J., Miralles A., Tariq A., et al. (2024). Growing aridity poses threats to global land surface. Communications Earth & Environment, 5, 776. https://doi.org/10.1038/s43247-024-01935-1

Serdyanjiv N., Suzuki Y., Higurashi T., and Tanaka Y. (2024). Flood hazard mapping and disaster-prevention recommendations based on detailed topographical analysis in Khovd City, Western Mongolia. Natural Hazards and Earth System Sciences Discussions (preprint). https://doi.org/10.5194/nhess-2024-91

Shestakova T.A., Gutiérrez E., Kirdyanov A.V., Camarero J.J., Génova M., Knorre A.A., Linares J.C., Resco de Dios V., Sánchez-Salguero R., and Voltas J. (2016). Forests synchronize their growth in contrasting Eurasian regions in response to climate warming, Proc. Natl. Acad. Sci., 113 (3), 662-667. https://doi.org/10.1073/pnas.1514717113

Shestakova T.A., Gutiérrez E., Valeriano C., Lapshina E., and Voltas J. (2019). Recent loss of sensitivity to summer temperature constrains tree growth synchrony among boreal Eurasian forests. Agricultural and Forest Meteorology, 268, 318–330. https://doi.org/10.1016/j.agrformet.2019.01.039

Shigimaga, A.A., Bykov, N.I. and Rygalova, N.V. (2024). Features of Radial Growth of Trees in Shelterbelts of the Dry Steppe. Arid Ecosyst., 14, 463–472. https://doi.org/10.1134/S2079096124700434

Tabakova M., Arzac A., Martínez E., and Kirdyanov A. (2020). Climatic factors controlling Pinus sylvestris radial growth along a transect of increasing continentality in southern Siberia. Dendrochronologia, 62, 125709. https://doi.org/10.1016/j.dendro.2020.125709

Tejedor E., Serrano-Notivoli R., de Luis M., et al. (2020). A global perspective on the climate-driven growth synchrony of neighboring trees. Global Ecology and Biogeography, 29(7), 1114-1125. DOI:10.1111/geb.13090

Tsydypov B.Z., Garmaev E.Zh., Gomboev B.O., et al. (2022). Impact of climate change on ecosystem services of forest lands in the south of Eastern Siberia. Izvestiya RAN. Seriya Geograficheskaya, 86(1), 82–97. https://doi.org/10.31857/S2587556622010125 (In Russian).

Vaganov E.A., Shiyatov S.G., Mazepa V.S. (1996). Dendroclimatic study in Ural-Siberian Subarctic. Novosibirsk: Nauka Publ., 248 pp. (In Russian).

Van Der Schrier G., Barichivich J., Briffa K.R., and Jones P.D. (2013). A scPDSI-based global data set of dry and wet spells for 1901-2009. J. Geophys. Res. Atmos. 118, 4025–4048. doi: 10.1002/jgrd.50355

Voropay N.N., Ryazanova A.A. (2023). Changes in hydrothermal conditions in Southern Siberia in 1950–2020 and their relation to large-scale circulation processes. Russian Meteorology and Hydrology, 48(10), 897–904. https://doi.org/10.3103/S1068373923100096

Wang H., Zuo Z., Qiao L., et al. (2022). Frequency of winter temperature extremes over Siberia dominated by the Atlantic Meridional Overturning Circulation. npj Climate and Atmospheric Science, 5, 84. https://doi.org/10.1038/s41612-022-00307-w

Wang X., Xie F., Zhang Z., et al. (2021). Complex network of synchronous climate events in East Asian tree-ring data. Climatic Change, 165, 54. https://doi.org/10.1007/s10584-021-03008-0

Wilhite D.A., Glantz M.H. (1985). Understanding the drought phenomenon: The role of definitions. Water International, 10(3), 111–120. https://doi.org/10.1080/02508068508686328

Zadonina N.V., Levi K.G. (2008). Chronology of natural and social phenomena in Siberia and Mongolia: A monograph. Irkutsk: Irkutsk State University Press, 759 pp. (In Russian).